Journal of Materials Chemistry C

Accepted Manuscript

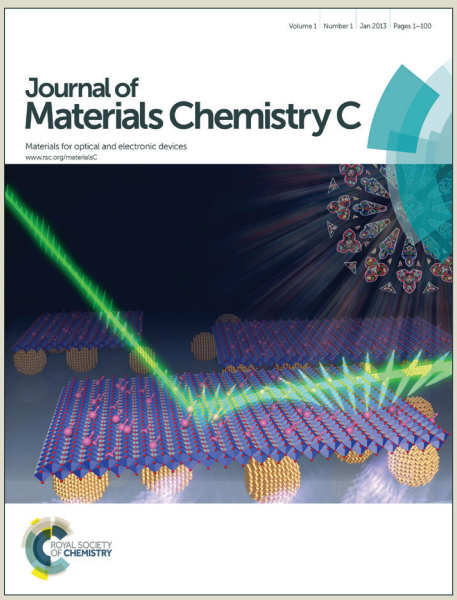

ROYAL SOCIETY OF CHEMISTRY

www.rsc.org/materialsC

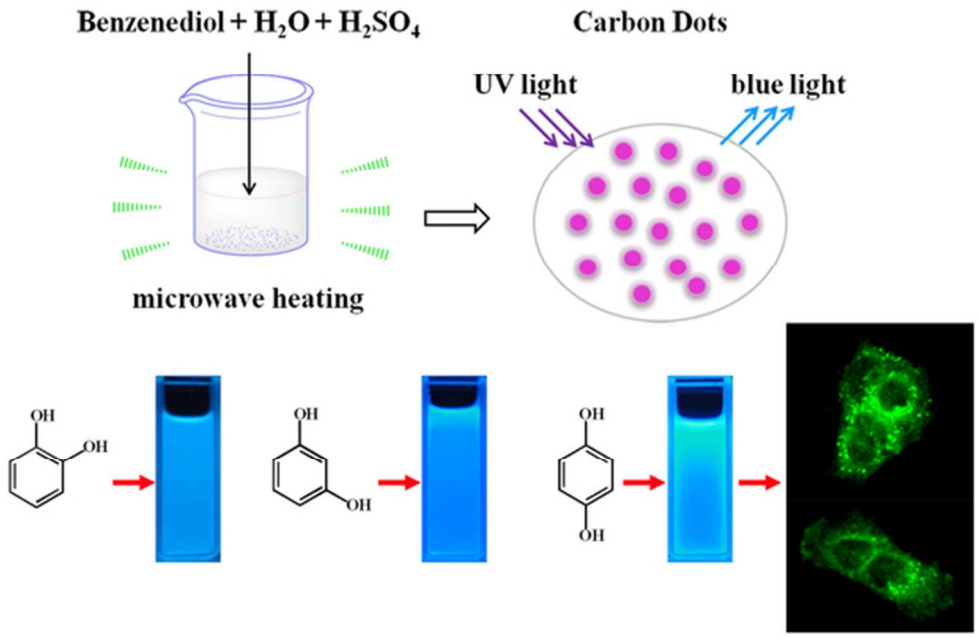

Diagram of preparation of CDs and photographs of the fluorescent Carbon Dots solution and bioimaging
53x36mm (300 x 300 DPI)

Cite this: DOI: 10.1039/c0xx00000x

www.rsc.org/xxxxxx

ARTICLE TYPE

A facile large-scale microwave synthesis of highly fluorescent carbon dots from benzenediol isomers

Jun Wang,[a] Changming Cheng,[a] Ying Huang,[a] Baozhan Zheng,[b] Hongyan Yuan,[a] Lin Bo,[c] Ming-Wu Zheng,[d] Sheng-Yong Yang,[d] Yong Guo[b,*] and Dan Xiao[a,b,*]

Received (in XXX, XXX) Xth XXXXXXXXX 20XX, Accepted Xth XXXXXXXXX 20XX
DOI: 10.1039/b000000x

A fast large-scale synthesis of fluorescent carbon dots (CDs) has been developed in this work without high temperature or high pressure. Using benzenediol (catechol, resorcinol and hydroquinone) as the carbon precursor, sulfuric acid as the catalyst, three distinct CDs with strong and stable luminescence were prepared via microwave-assisted method within 2 min. Characterizations through high-resolution transmission electron microscopy, X-ray diffraction, elemental analysis and infrared spectroscopy indicated the as-prepared CDs are dispersed spherical oxygenous carbon nanoparticles with 0.5-6 nm in size. The structure difference caused by isomer precursors was reflected in the chemical and fluorescent properties of CDs. The quantum yields of the three kinds of CDs derived from catechol, resorcinol and hydroquinone are 9.2%, 42.8% and 26.5%, respectively. The fluorescence lifetime of these CDs are in nanosecond scale. And the one derived from hydroquinone could easily penetrate into the cells in a short time (30 min) and possess low cytotoxicity and good biocompatibility which may have great potential for bioimaging application.

1 Introduction

In the past few years, fluorescent carbon dots (CDs) or graphene quantum dots (GQDs) have drawn a lot of attention because of the photostability, biocompatiblility, lower environmental hazard compared to traditional heavy-metal-based quantum dots.[1, 2] Various works have demonstrated a promising application potential of CDs in bioimaging,[3-9] light-emitting devices,[10] sensors,[11, 12] and photovoltaics.[13-15] Until now, a great many of methods have been explored for the preparation of fluorescent CDs and GQDs, for instance, arc-discharge,[16] chemical oxidation,[5, 17-21] electrochemical oxidation,[1, 15, 22-25] pyrolysis,[26-29] laser ablation,[30, 31] hydrothermal method,[7, 19, 32, 33] and template approach,[34] which could be classified into top-down and bottom-up routes. These methods usually involve tedious processes, expensive devices, or harsh synthetic conditions (strong acid, strong oxidant, ice bath, or high temperature and pressure). Most reported quantum yields (QY) for carbon nanoparticles are relatively low, often less than 10%. To enhance the QY of CDs, surface passivation, doping with heteroatom like nitrogen and size control demonstrate to be available in some degree.[3, 6, 8, 9, 35-38] However, it is still a challenge to take account of easy preparation, large-scale synthesis and high quantum yield in one method.

Microwave-assisted techniques have been widely applied for the materials synthesis because it could provide simultaneous, homogeneous and efficient heating, and lead faster reaction rate and uniform size distribution of product. Our group reported a facile and large-scale synthesis of the mesoporous α–$Ni(OH)_2$ via microwave-assisted heating.[39] Among all the CDs synthesis routes, microwave-assisted method seems to be the most facile, time-saving and cost-effective way.[40-43] The report of fluorescent carbon nanoparticles fabricated in the dehydration of acetic acid,[44] inspired us that carbonization might be an efficient way for the preparation of CDs. Bottom-up synthesis is a good strategy to control the CDs' size which is very essential to obtain high QY.[34] There have been a lot of bottom-up methods, reported various small organic molecules used as carbon precursors, including acids, amines, carbohydrates, alcohols and amino acid.[8, 9, 26-29, 33, 35, 36, 38, 40, 41, 43, 45, 46] As well known, molecules with rigid structure probably show strong fluorescence. We anticipate that a small molecule with the aromatic ring and hydroxyl group used as carbon source might result into highly fluorescent CDs, since the aromatic ring is easy to form co-plane structure and the hydroxyl group is needed for dehydration and introduction of oxygenous defects. Recently, R. Liu *et al.* reported a soft-hard template approach for preparing photoluminescent CDs using 1,3,5-trimethylbenzene, diaminebenzene, pyrene and phenanthroline as carbon sources with QYs of 3.3%-4.7%.[34] X. Feng and X. Yin *et al.* prepared CDs with the carbonization-extraction strategy and the HNO_3 refluxing method using 3-(3,4-dihydroxyphenyl)-*L*-alanine (*L*-DOPA) as carbon source with QYs of 6.3% and 1.0%.[47] X. Qu *et al.* reported a hydrothermal synthesis of luminescent CDs from dopamine with a QY of 6.4%.[48] Herein, we report a new method for the large-scale synthesis of strongly luminescent CDs. Catechol, resorcinol and hydroquinone are dissolved in water respectively, only add a small amount of sulfuric acid as the

catalyst, and then three distinct CDs are obtained via microwave heating (see Figure 1). Characterizations indicated as-prepared CDs are dispersed spherical oxygenous carbon nanoparticles with 0.5-6 nm in size.

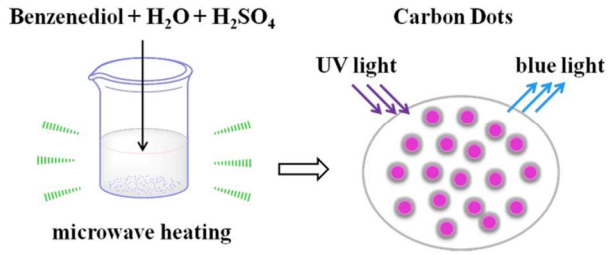

Figure 1. Diagram of preparation of the fluorescent CDs.

2 Experiment

2.1 Materials

Catechol (*o*-$C_6H_6O_2$), resorcinol (*m*-$C_6H_6O_2$), hydroquinone (*p*-$C_6H_6O_2$), sulfuric acid (H_2SO_4), ethanol (C_2H_5OH) and 1-butanol were purchased from Kelong Chemicals Co., Ltd. (Chengdu, China). Quinine sulfate was purchased from J&K CHEMICAL (Beijing, China). All other reagents were of analytical grade and used as received without any further purification. Double distilled water (DDW) was used throughout.

2.2 Preparation of CDs

The fluorescent CDs were synthesized via a microwave-assisted method in homogeneous sulfuric acid conditions. Typically, 1.000 g *m*-$C_6H_6O_2$ and 100 μL H_2SO_4 were dissolved in 2 mL DDW. Then the mixture solution was heated in a domestic microwave oven (maximum power 800 W, 2450 MHz) for 20-120 s. After that, the volume of the solution decreased since most of the water evaporated, and the color changed into wine red. After cooling to room temperature, the crude product was added 50 mL each of 1-butanol and DDW to separate fluorescent CDs via extraction. The pH of the water was neutral after several times of extraction with DDW. Then the 1-butanol was extracted by a rotary evaportaor under the vacuum condition at ~60℃. Finally, the product was dried in a vacuum oven at 60℃ overnight to get a solid product or dispersed in ethanol or DDW for further characterization. For the other two kinds of CDs, the preparation process was similar just the ratio of the reactant and time were different: 1.000 g *o*-$C_6H_6O_2$ and 200 μL H_2SO_4 were dissolved in 2 mL DDW, and heated in the microwave oven for 20-120 s; 0.500 g *p*-$C_6H_6O_2$ and 200 μL H_2SO_4 were dissolved in 4 mL DDW, and heated in the microwave oven for 10-50 s.

2.3 Characterization

UV-vis absorption spectra were recorded on a Techcomp UV1100 UV-visible absorption spectrophotometer (Beijing, China) at room temperature. Fluorescence spectra were measured on a HITACHI F-7000 fluorescence spectrometer (Tokyo, Japan). The photomultiplier tube (PMT) voltage was set at 700 V. X-ray photoelectron spectroscopy (XPS) was conducted on a Kratos XSAM 800 photo-electron spectrometer (Manchester, UK). Fourier transform infrared spectroscopy (FT-IR) characterization was carried out on a Thermo Nicolet 6700 FT-IR spectrophotometer (Vernon Hills, Illinois, USA). The transmission electron microscopy (TEM) and high resolution TEM (HRTEM) images were obtained by an FEI Tecnai F-20 field emission HRTEM (Hills-boro, OR, USA) operating at 200 kV. X-ray diffraction (XRD) measurement was acquired on a Tongda TD-3500 X-ray powder diffractometer (Liaoning, China) with Cu Kα radiation (λ=0.154 nm). The XRD pattern was recorded from 5°-80° at a scan rate of 0.06°/s. Elemental analysis was carried out using a Thermo Finnigan FLASH 1112 SERIES CHNS-O analyzer (USA). The lifetime measurements were performed on a HORIBA TemPro 01 fluorescence lifetime system (Glasgow, UK). A 370 nm NanoLED pulsed diode excitation source was used to excite the samples.

2.4 Cell incubating

The living L02 cell was provided by Regenerative Medicine Research Center, West China Hospital, Sichuan University (Sichuan, China). The L02 cells were incubated with high glucose medium (H-DMEM) (Gibco, USA) supplemented with 10% fetal calf serum (FBS) (Gibco, USA) for 48 h at 37ºC. Then, CDs PBS solution was introduced to the cell culture medium. After incubation for 30 min, the L02 cells were washed three times with PBS (1000 μL each time), and then imaged by laser scanning confocal microscope (LSCM, Nikon A1) with the excitation wavelength 405 nm and 488 nm.

2.5 MTT assay

Cytotoxicity was evaluated by MTT assay as previously described.[49] Cells were seeded onto 96-well plates, including Hela cells and MCF-7 cells. After a 24-h incubation in serum-containing media, cells were treated with 200 μL indicated concentrations of *o*-CDs, *m*-CDs and *p*-CDs for 72 h in serum-containing media. Then, 20 μL of 5 mg/mL MTT solution (Sigma, St. Louis, MO) was added to each well and plates were incubated for 2 h at 37℃. After carefully aspirating the media and MTT from each well, the formazan crystals were dissolved with 150 μL of DMSO (Sigma, St. Louis, MO), and absorbance was read at 570 nm with an Multiscan MK3 microplate reader (Thermofisher Inc.). Each assay was replicated 3 times. Cells without treatment with CDs were taken as a control.

3 Results and Discussion

In this work, the small oxygenous aromatic molecules benzenediol isomers were selected as the carbon precursor for the fabrication of CDs. The products were named *o*-CDs, *m*-CDs and *p*-CDs for the precursors catechol (*o*-$C_6H_6O_2$), resorcinol (*m*-$C_6H_6O_2$) and hydroquinone (*p*-$C_6H_6O_2$), respectively. In our preliminary work, sulfuric acid was used as both dehydrator and solvent in the microwave heating reaction. Unfortunately, only a few fluorescent CDs could be obtained since most of the reactant turned to carbon block in the concentrated sulfuric acid. Alternatively, diluted sulfuric acid was used instead of concentrated one, resulting in a large amount of fluorescent CDs. After microwave-assisted heating, the color of the mixture solution turned to wine red or dark red or dark green, indicating

the formation of the carbon dots. To find the optimal volume of H_2SO_4, 1000 μL, 500 μL, 100 μL and 50 μL were added into the solution of 1.000 g *m*-$C_6H_6O_2$ and 2 mL H_2O, respectively. The one added 1000 μL H_2SO_4 trended to carbonize; the ones added 500 μL and 100 μL H_2SO_4 could both obtain a lot of CDs in 40 seconds; the one added 50 μL H_2SO_4 obtained fewer CDs in the same time. As a result, we chose the match of 1.000 g *m*-$C_6H_6O_2$, 2 mL H_2O and 100 μL H_2SO_4. Besides, some other acid like hydrochloric acid, nitric acid and phosphoric acid were tried as the catalyst instead of sulfuric acid. Enhancing the quantity and the microwave time, the same fluorescent product was only observed in the one added phosphoric acid. But the yield of product using phosphoric acid as catalyst was low, not as much as that using sulfuric acid.

Then, the effect of microwave time on the preparation of CDs was investigated. Taking the synthesis of *m*-CDs for instance, 1.000 g *m*-$C_6H_6O_2$ and 100 μL H_2SO_4 were dissolved in 2 mL DDW. As shown in Figure S1, with the increase in microwave time, the light yellow transparent mixture solution turned to orange in first 20 s, then wine red after 30 s, and dense solution after 40 s. No more visible difference among products heated for 40-120 s was observed. After abstraction and oven dry, the output of *m*-CDs heated for 40-120 s were 0.490-0.823 g (see in Table S1). The time point of maximum yield appears at 100 s.

For the synthesis of *o*-CD, we chose the match of 1.000 g *o*-$C_6H_6O_2$, 2 mL H_2O and 100 μL H_2SO_4 at first. With the solution decreased during the microwave heating, *o*-$C_6H_6O_2$ mostly crystallized before turning into CDs. That's because the solubility of *o*-$C_6H_6O_2$ in water is not as good as *m*-$C_6H_6O_2$. So we adjusted the match to 0.500 g *o*-$C_6H_6O_2$, 2 mL H_2O and 100 μL H_2SO_4. As seen in figure S2, the change appeared after heating for 20 s; obvious dark red materials showed up after 30 s; no more visible difference among products heated for 40-120 s was observed in naked eyes. But some crystals appeared in the products heated for 30-60 s after cooling to room temperature which implies that part of the precursor didn't react. And the output of *o*-CDs prepared for 70-120 s was 0.172-0.206 g (Table S2).

The solubility of *p*-$C_6H_6O_2$ in water is even poorer than *o*-$C_6H_6O_2$ that 0.500 g *p*-$C_6H_6O_2$ couldn't dissolve in 4 mL DDW. We utilized microwave energy to make *o*-$C_6H_6O_2$ dissolved and increased the amount of H_2SO_4 to accelerate the reaction. As seen in figure S3, 0.500 g *p*-$C_6H_6O_2$ and 200 μL H_2SO_4 were dissolved in 4 mL DDW completely after heating for 10 s; the solution decreased and turned a little pink after 30 s, the color change means a few CDs had generated already; the solution changed to dark green after 40 s which implies numerous CDs had formed; carbonization was observed after 50 s. The optimum microwave time for *p*-CDs is 40 s. The output of *p*-CDs prepared for 40 s was 0.110 g.

Since the as-prepared CDs were found to be well dissolved in 1-butanol, the pure CDs were obtained via extracting against water to remove the acid for a series of characterizations of the CDs. The transmission electron microscope (TEM) images are shown in Figure 2, revealing that the particles are dispersed without apparent aggregation and possess a nearly spherical shape, with diameters of 0.5-6 nm. The average sizes of *o*-CDs, *m*-CDs and *p*-CDs are 3.5 nm, 1.9 nm and 2.8 nm, respectively. The high resolution TEM (HRTEM) images (inset of Figure 2) clearly unveil the crystal lattice of *o*-CDs, *m*-CDs and *p*-CDs, the spacing of which are calculated to be 0.217 nm, 0.212 nm and 0.211 nm, respectively, close to the d-spacing of the (1100) facet of graphite (0.213 nm).[50, 51] The corresponding X-ray diffraction (XRD) pattern, shown in Figure S4, displays a broad (002) peak centered at ca. 25°, which is similar to CDs and GQDs fabricated by other methods.[28, 43]

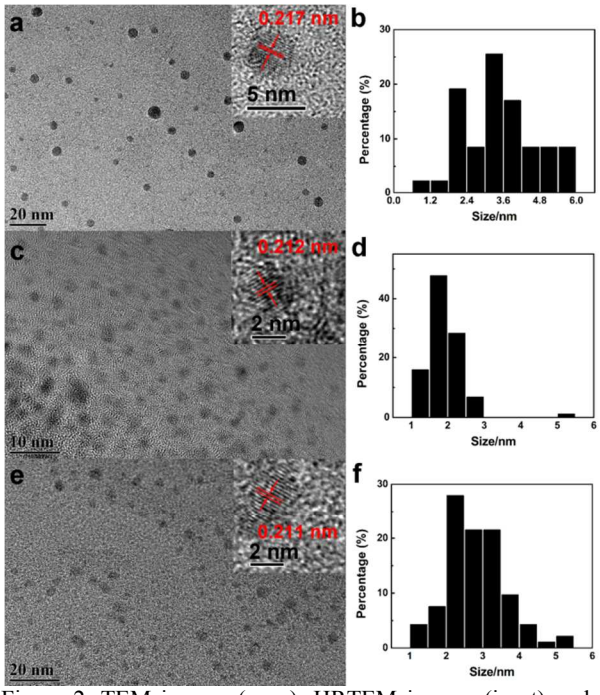

Figure 2. TEM images (a,c,e), HRTEM images (inset) and size histogram (b,d,f) of the *o*-CDs (a,b), *m*-CDs (c,d) and *p*-CDs (e,f).

The X-ray photoelectron spectrometry (XPS) measurements were carried out to probe the composition of CDs. As seen in Figure 3, the XPS spectrum of *o*-CDs shows dominant O1s peak at 535.2 eV and C1s peak at 287.5 eV. In detail, the C1s spectrum shows three peaks at 284.6 eV, 285.5 eV and 287.0 eV, correspond to C-C, C-O and C=O, respectively. The spectrum of *m*-CDs shows dominant O1s peak at 534.5 eV and C1s peak at 286.2 eV. In the C1s spectrum of *m*-CDs, three peaks at 284.6 eV, 285.6 eV and 287.1 eV are shown, corresponding to C-C, C-O and C=O, respectively. The XPS spectrum of *p*-CDs shows dominant O1s peak at 535.8 eV and C1s peak at 288.2 eV. In the C1s spectrum of *p*-CDs, three peaks at 284.6 eV, 285.5 eV and 287.0 eV are also shown, correspond to C-C, C-O and C=O, respectively. The results reveal that the as-prepared CDs contains mainly carbon and oxygen, indicating sulfuric acid only plays the role of catalyst. The C-O/C=O of CDs are shown in Table S3. It's clear that the proportion of C-O is much more than C=O which might explain why those as-prepared CDs are much better dissolved in alcohol than in H_2O.

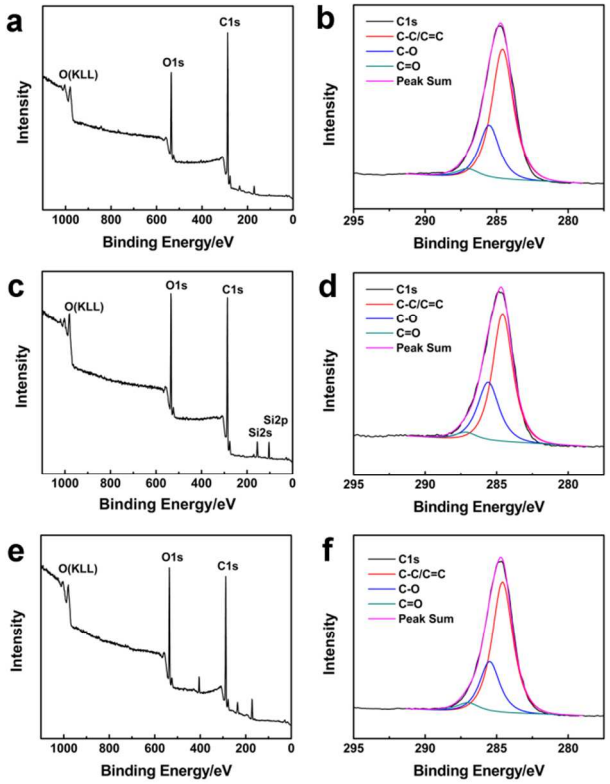

Figure 3. XPS and C1s spectra of *o*-CDs (a,b), *m*-CDs (c,d) and *p*-CDs (e,f).

Table 1. Elemental analysis results of *o*-CDs, *m*-CDs and *p*-CDs.

samples	elemental analysis		
	C (wt%)	H (wt%)	O (wt%, calculated)
o-CDs	63.6	2.5	33.9
m-CDs	70.5	3.7	25.8
p-CDs	70.3	2.8	26.9

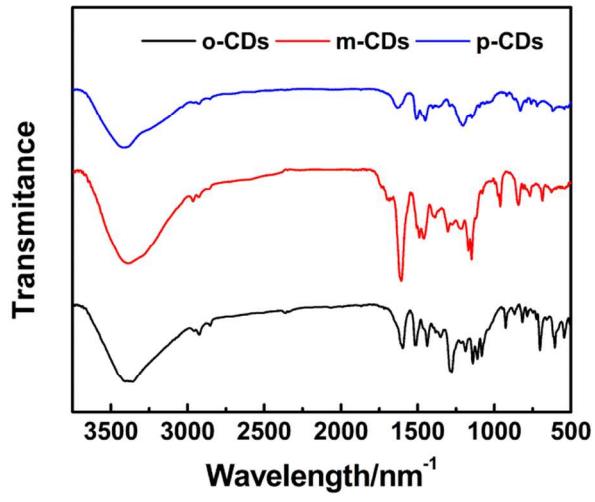

Figure 4. Typical FTIR spectra of *o*-CDs (black), *m*-CDs (red) and *p*-CDs (blue).

The elemental analysis results shown in Table 1 indicate that the carbon contents of *m*-CDs and *p*-CDs are higher than the precursors (calculated to be ~65.45%), implying that the benzenediol precursors should be carbonized in some degree during the microwave-assisted pyrolysis. *o*-CDs have lower carbon content and higher oxygen content, while the hydrogen content is close to that of *p*-CDs. The higher oxidation degree of *o*-CDs indicates that there might be oxidation in some degree during carbonization.

Furthermore, Fourier transform infrared (FTIR) spectra were acquired to determine the surface state of CDs. As shown in Figure 4, the as-prepared *o*-CDs exhibited characteristic absorption bands of stretching vibration of O-H (ν_{O-H}) at 3358 cm^{-1}, stretching vibration of C=O ($\nu_{C=O}$) at 1596 cm^{-1}, skeletal vibration of aromatic ring ($\nu_{C=C}$) at 1509 cm^{-1} and 1437 cm^{-1}, and stretching vibration of C-O (ν_{C-O}) at 1277 cm^{-1} and 1110 cm^{-1}. While for *m*-CDs, characteristic absorption bands of ν_{O-H} at 3385 cm^{-1}, $\nu_{C=O}$ at 1684 cm^{-1} and 1607 cm^{-1}, $\nu_{C=C}$ at 1489 cm^{-1} and 1458 cm^{-1}, and ν_{C-O} at 1168 cm^{-1} and 1148 cm^{-1} are found. Similarly, characteristic absorption bands of ν_{O-H} at 3419 cm^{-1}, $\nu_{C=O}$ at 1629 cm^{-1}, $\nu_{C=C}$ at 1508 cm^{-1} and 1450 cm^{-1}, ν_{C-O} at 1203 cm^{-1} and 1146 cm^{-1} are found in the FTIR spectrum of *p*-CDs. These results which are similar to the previous reports,[30, 40, 52] indicate there are oxygen-containing functional groups in the CDs corresponding to the XPS measurement.

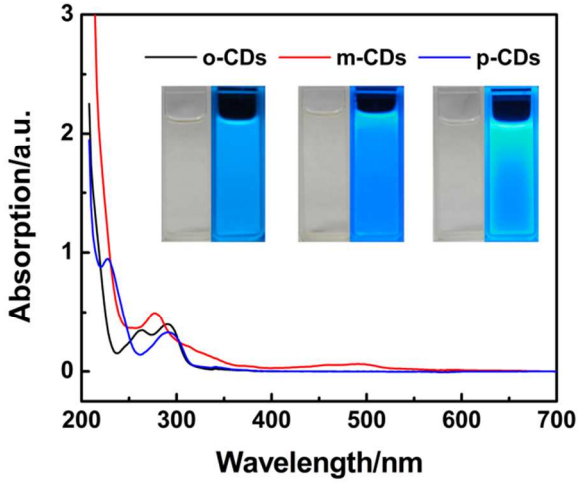

Figure 5. UV-Vis absorption of *o*-CDs (black), *m*-CDs (red) and *p*-CDs (blue). Inset: photographs of the *o*-CDs , *m*-CDs and *p*-CDs solution (0.02 mg/mL) taken under visible light (left) and 365 nm UV light (right).

To study the optical properties of the CDs, UV–vis absorption and PL studies were carried out in detail. As illustrated in Figure 5, absorption spectra of *o*-CDs, *m*-CDs, *p*-CDs exhibit peaks at 264/290 nm, 276 nm, 291 nm, respectively, which are ascribed to the typical absorption of the n–π* transition of C=O.[10, 31, 37, 43] Besides, absorption spectrum of o-CDs exhibits the absorption bands at 228 nm which are from the π–π* transition of C=C of the polyaromatic sp^2-hybrid carbon network.[10, 20, 43] Insets of Figure 5 are the photographs of CDs dispersion taken under visible and UV lights. The bright blue fluorescent color in the dilute solutions could be observed clearly with naked eyes under

a UV lamp.

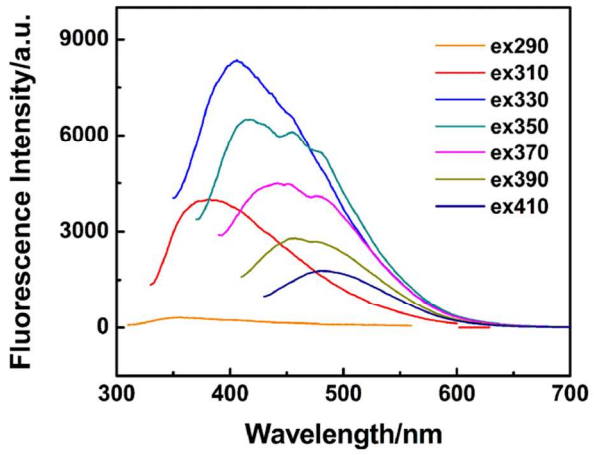

Figure 6. PL spectra of *o*-CDs ethanol solution (0.02 mg/mL).

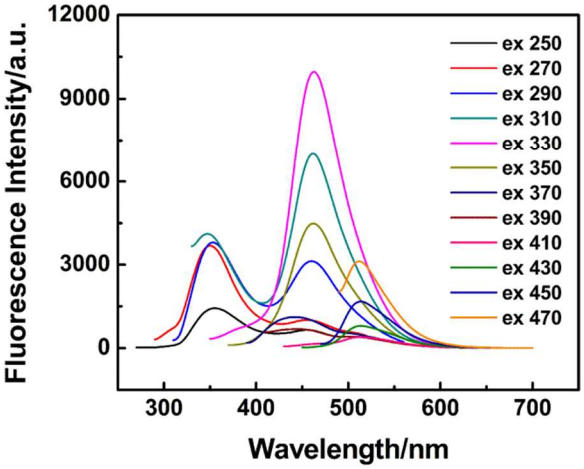

Figure 7. PL spectra of *m*-CDs aqueous solution (0.02 mg/mL).

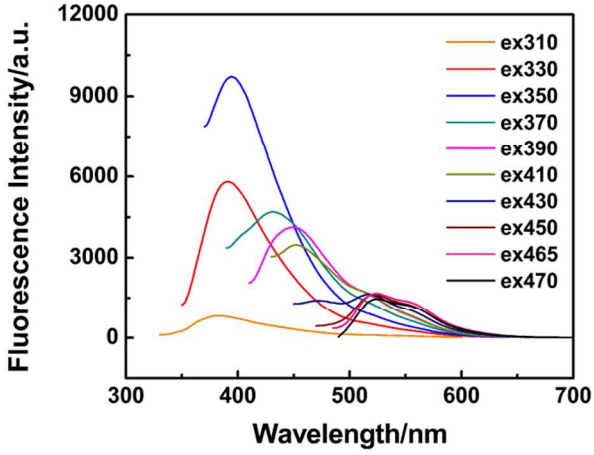

Figure 8. PL spectra of *p*-CDs ethanol solution (0.02 mg/mL).

A detailed photoluminescence (PL) study was carried out by using different excitation wavelengths. An excitation-dependent PL is seen in the PL spectra of *o*-CDs (Figure 6). The emission peak shifts from *ca.* 350 nm to *ca.* 500 nm while excitation wavelength changes from 290 to 410 nm, which is similar with the most CDs in the previous literatures.[6, 7, 19, 27, 33, 37, 38] The excitation-dependent PL is associated with the inhomogeneous ultrafine size and surface state with a high concentration of structure defect sites. The maximum excitation and emission peaks of *o*-CDs are at *ca.* 330 and 400 nm. The PL spectra of *m*-CDs are broad and change with the varied excitation wavelengths. Unlike most other fluorescent CDs, the *m*-CDs doesn't exhibit a normal excitation-dependent PL behavior. When the excitation wavelength changes from 250 to 470 nm (Figure 7), three emission peaks at *ca.* 350, 470 and 520 nm show up in sequence which nearly don't shift only the intensity changed. Additionally, the emission peaks around *ca.* 350 and 470 nm exist at the same time during excitation wavelength changed from 250 to 310 nm. The maximum emission peak of *m*-CDs at *ca.* 460 nm was observed while excited at 330 nm. The excitation-independent PL of GQDs reported in previous literature,[28] implies that both the size and the surface state of those sp^2 clusters contained in GQDs should be uniform. The observed PL phenomenon of as-prepared *m*-CDs has not yet been reported. There may be three dominated species of surface state of sp^2 clusters contained in *m*-CDs. The solubility of *m*-CDs in water is not as good as in alcohol, but the *m*-CDs aqueous solution still exhibits strong luminescence. The *p*-CDs possess different PL spectra from both *o*-CDs and *m*-CDs (Figure 8). When the excitation wavelength changed from 310 to 430 nm, the excitation-dependent PL was observed. While excitation wavelength changed from 430 to 470 nm, emission peaks at *ca.* 520 and 560 nm show up. The maximum emission and excitation peaks of *p*-CDs were at *ca.* 400 and 350 nm.

Using quinine sulfate as a standard, we measured the quantum yield of the CDs prepared from three precursors (Figure S6, Table S4). The quantum yields of *o*-CDs, *m*-CDs and *p*-CDs are 9.2%, 42.8% and 26.5%, respectively. The as-prepared *m*-CDs and *p*-CDs possess higher QY than most reported non-doping CDs (mostly <20%) without any surface passivation or heteroatom (like N, S or P) doping, even higher than some reported nitrogen-doping CDs.[6, 8, 34, 35, 37] To enhance the QY of CDs, nitrogen-doping has become popular.[8, 36, 38] From another point of view, we may not say that the amino group is the essential route to obtain highly luminescent CDs. The photostability of CDs was also tested by monitoring the change of the emission intensity with irradiation time using the Xe light. After irradiation for 9000 s (2.5 h), no obvious PL bleaching is observed and the signals are strong and stable (Figure S5). The results signify the excellent reversibility of the PL signal, inferring its potential as a fluorescent marker. It was found to be possible to re-disperse the dry sample in alcohol easily without any aggregation, which is significant for preservation and transportation.

The time-resolved fluorescence decay curves measured by time-correlated single photon counting method are illustrated in Fig S7-9. The decay curve of *o*-CDs can be very well fitted to a triple-exponential function. As seen in Table S5, the lifetimes of *o*-CDs are τ_1 = 0.42 ns (~27%), τ_2 = 1.97 ns (~51%) and τ_3 = 6.05 ns (~22%), and the mean lifetime is calculated to be 2.43 ns. The decay curve of *m*-CDs can be very well fitted to a single-exponential function and the lifetime is 4.95 ns (100%). Similar to *o*-CDs, the decay curve of *p*-CDs can be very well fitted to a

triple-exponential function. The average lifetime of *p*-CDs is 1.64 ns and contains three lifetime components of 0.30 ns (~14%), 1.23 ns (~49%) and 2.69 ns (~37%). The results are in line with the previous reports.[21, 52] All the CDs have a short lifetime which indicates that the possible luminescent mechanism is the radioactive recombination nature of excitations.[40, 52]

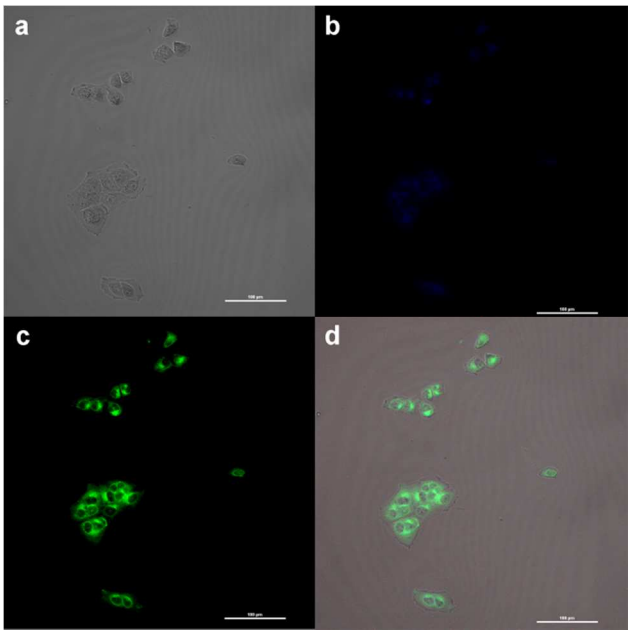

Figure 9. Laser scanning confocal microscopy images of L02 cells incubated with *p*-CDs (200 μg/mL) for 30 min after washing with 0.2 M PBS: (a) bright field, (b) fluorescent images excited with a 405 nm laser, (c) fluorescent images excited with a 488 nm laser, (d) merged image of a, b and c.

The observed lifetime of CDs in nanosecond indicates that the synthesized CDs are suitable for optoelectronic as well as biological applications. The *in vitro* cellular uptake and bioimaging experiments of the CDs in L02 cell were performed. It's interesting that among the three kinds of CDs only the *p*-CDs could be gathered in the cells. Upon incubation with the *p*-CDs in a culture medium at 37℃ only for 30 min, the L02 cells became brightly illuminated when imaged on the fluorescence microscope with excitation by 405 nm and 488 nm laser pulses, and still maintained the fine shape. After washing with 0.2 M PBS three times, the L02 cells still emitted blue and green fluorescence when excited by 405 nm and 488 nm laser pulses, as shown in Figure 9. We could see the *p*-CDs are able to label the cytoplasm of L02 cells without reaching the nucleus in a significant fashion which means no genetic disruption would occur. Specifically, the green bright spots in the cytoplasm are shown in Figure S10, implying the *p*-CDs might prefer to gathering in the organelles like mitochondria. Comparison between (a) and (b) of Figures S10, it can be seen that the blue emission from aggregated cell clusters is stronger than the two and three closed cells; however, the green emission from them is much the same. That implies the blue and green light might come from different nanoparticles. The CDs are mixture of fluorescent carbon nanoparticles with different defects. We could conclude there are at least two kinds of carbon nanoparticles in *p*-CDs that emit blue and green light. The blue one might have higher QY, and the green one might penetrate into the cells easier. It will be very important if the CDs could be used in biomedical application because of the good membrane penetrability and luminescence property. For future biological applications, the inherent cytotoxicity of the as-prepared CDs was tested using both Hela and MCF-7 cells by MTT assay. As shown in Figure 10, the viability of Hela cells retained more than 80% after treated with *p*-CDs at 33.33 μg/mL for 72 h, even at 100 μg/mL cell viability remained 75%; the viability of MCF-7 cells also retained more than 80% after treated with *p*-CDs at 33.33 μg/mL for 72 h. Compared to previously reported cytotoxicity of carbon nanoparticles and CdTe, the results suggests low cytotoxicity and good biocompatibility of *p*-CDs.[44]

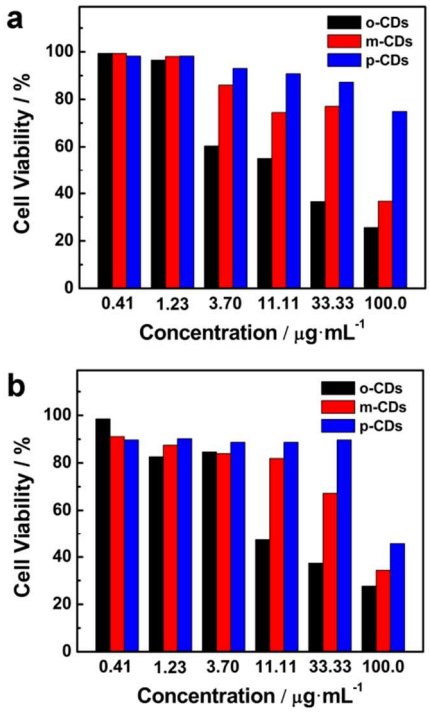

Figure 10. Cellular toxicity of CDs determined by MTT assay. Effect of different concentration of *o*-CDs, *m*-CDs and *p*-CDs on viability of Hela (a) and MCF-7 (b) cells, respectively.

A widely accepted mechanism for PL of CDs is the radioactive recombination of excitons.[3] Both of the size effect and surface defects contribute to the complexity of the excited states of CDs, the size effect is a result of quantum dimensions while the surface state is analogous to a molecular state.[6, 38, 53] Smaller CDs with the same or similar surface morphology and passivation are expected to achieve higher QY because of the quantum confinement of emissive energy traps to the particle surface.[3, 5] As shown in TEM images, the average size decreases in the order: *o*-CDs > *p*-CDs > *m*-CDs. The *m*-CDs possess the smallest average size and the biggest surface-to-volume ratio which facilitate the migration of photo-generated carriers. The XPS results imply the existence of large numbers of residual hydroxyl groups. As seen in Table S3, the *m*-CDs possess the highest C-

O/C=O among the three kinds of CDs. We speculate the ortho-, meta- and para-position substitution of the benzenediol groups at the surface of CDs could be regarded as self surface passivation, which may influence the surface state. It is reported that CDs synthesized by carbonizing *L*-DOPA have a relatively higher QY than the oxidized ones after refluxed in HNO_3, indicating the CDs with a low oxidation level have the high PL emission.[47] The elemental analysis results indicate the order of oxidation level is *o*-CDs > *p*-CDs > *m*-CDs. *o*-$C_6H_6O_2$ and *p*-$C_6H_6O_2$ are more easier to be oxidized to quinoid structure than *m*-$C_6H_6O_2$, contributing to less luminescence of as-derived *o*-CDs and *p*-CDs. The reduced PL might be connected with the increased oxidation level. The differences of molecular structure of carbon precursors might be one of the influence factors of PL properties and cell imaging application among *o*-CDs, *m*-CDs and *p*-CDs. For different isomer precursors, chemical property determined by structure affects the ease of reaction and different bonding sites which result in different structure defects. The meta-substitution of the precursor makes the derived *m*-CDs special. The electron transmission of *m*-$C_6H_6O_2$ is different from that of *o*-$C_6H_6O_2$ and *p*-$C_6H_6O_2$, and is harder to spread energy through conjugation, which decides the electron transfer and energy release path of *m*-CDs leans to radiate through luminescence. Thus, the combined effect of above-mentioned reasons may determine the *m*-CDs possess the highest quantum yield. The *p*-CDs could penetrate the cell membrane easily, not the *o*-CDs or *m*-CDs, may ascribe to the surface structure of *p*-CDs. As shown in Figure 11, *p*-CDs are more hydrophobic than the other two. That makes the *p*-CDs be more suitable for cell imaging.

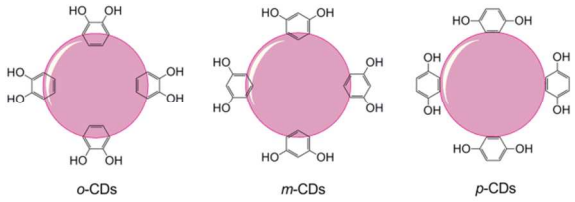

Figure 11. Schematic representation of benzenediol groups at the surface of *o*-CDs, *m*-CDs and *p*-CDs, respectively.

The CDs are mixture of fluorescent carbon nanoparticles with similar structure. They may possess diverse substituted oxygenous groups or different oxidation degree, but could be classified into the same category because of the same basic structure, just like the graphene oxide and graphene quantum dots. We try to study further *via* the separation of as-prepared CDs through the high performance liquid chromatography. And the detail research will be reported elsewhere.

Conclusions

We found a way for one-step synthesis of highly fluorescent CDs by microwave-assisted method using benzenediol as carbon source and sulfuric acid as catalyst. It provides a feasible route of mass production. The as-prepared CDs were characterized to be dispersed 0.5-6 nm oxygenous carbon nanoparticles. Due to the structure difference of precursor, CDs prepared with the same synthesis method possess different properties. The *m*-CDs derived from resorcinol emit blue fluorescence with quantum yield as high as 42.8% without any surface passivation or heteroatom (like N, S or P) doping. The *p*-CDs derived from hydroquinone with QY 26.5% could easily penetrate into the cells in a very short time, and possess low cytotoxicity and good biocompatibility. We presume the *p*-CDs would be an attractive candidate in bioimaging field.

Acknowledgement

This work is supported by the National Natural Science Foundation of China (NSFC) (No. 21175083, 21175094, 21177090, 21275104) and the Doctoral Program Foundation of Institutions of Higher Education of China (No. 20120181120075).

Notes and references

[a] *College of Chemical Engineering, Sichuan University, No.24 South Section 1, Yihuan Road, Chengdu 610065, P. R. China. Fax: +86-28-85415029; Tel: +86-28-85416029; E-mail: xiaodan@scu.edu.cn*
[b] *College of Chemistry, Sichuan University, No.29 Wangjiang Road, Chengdu 610064, P. R. China. Fax: + 86-28-85412907; Tel: + 86-28-85416218; E-mail: guoy@scu.edu.cn*
[c] *Regenerative Medicine Research Center, West China Hospital, Sichuan University, No.1 Keyuan Road Four, Chengdu 610041, P. R. China.*
[d] *State Key Laboratory of Biotherapy and Cancer Center, West China Hospital, West China Medical School, Sichuan University, Chengdu 610041, P. R. China.*

† Electronic Supplementary Information (ESI) available: [details of any supplementary information available should be included here]. See DOI: 10.1039/b000000x/

1. Q. Zhao, Z. Zhang, B. Huang, J. Peng, M. Zhang and D. Pang, Chem. Commun., 2008, 0, 5116-5118.
2. S. Yang, X. Wang, H. Wang, F. Lu, P. G. Luo, L. Cao, M. J. Meziani, J. Liu, Y. Liu and M. Chen, J. Phys. Chem. C, 2009, 113, 18110-18114.
3. Y. P. Sun, B. Zhou, Y. Lin, W. Wang, K. A. Fernando, P. Pathak, M. J. Meziani, B. A. Harruff, X. Wang, H. Wang, P. G. Luo, H. Yang, M. E. Kose, B. Chen, L. M. Veca and S. Y. Xie, J. Am. Chem. Soc., 2006, 128, 7756-7757.
4. L. Cao, X. Wang, M. J. Meziani, F. Lu, H. Wang, P. G. Luo, Y. Lin, B. A. Harruff, L. M. Veca, D. Murray, S. Y. Xie and Y. P. Sun, J. Am. Chem. Soc., 2007, 129, 11318-11319.
5. S. Ray, A. Saha, N. R. Jana and R. Sarkar, J. Phys. Chem. C, 2009, 113, 18546-18551.
6. S. Zhu, J. Zhang, C. Qiao, S. Tang, Y. Li, W. Yuan, B. Li, L. Tian, F. Liu, R. Hu, H. Gao, H. Wei, H. Zhang, H. Sun and B. Yang, Chem. Commun., 2011, 47, 6858-6860.
7. D. Y. Pan, L. Guo, J. C. Zhang, C. Xi, Q. Xue, H. Huang, J. H. Li, Z. W. Zhang, W. J. Yu, Z. W. Chen, Z. Li and M. H. Wu, J. Mater. Chem., 2012, 22, 3314-3318.
8. X. Zhai, P. Zhang, C. Liu, T. Bai, W. Li, L. Dai and W. Liu, Chem. Commun., 2012, 48, 7955-7957.
9. C. W. Lai, Y. H. Hsiao, Y. K. Peng and P. T. Chou, J. Mater. Chem., 2012, 22, 14403-14409.
10. C. M. Luk, L. B. Tang, W. F. Zhang, S. F. Yu, K. S. Teng and S. P. Lau, J. Mater. Chem., 2012, 22, 22378-22381.
11. X. Zhang, H. Ming, R. Liu, X. Han, Z. Kang, Y. Liu and Y. Zhang, Mater. Res. Bull., 2013, 48, 790-794.
12. Y. Li, L. Zhang, J. Huang, R. Liang and J. Qiu, Chem. Commun., 2013, 49, 5180-5182.
13. X. Yan, X. Cui, B. Li and L. Li, Nano Lett., 2010, 10, 1869-1873.
14. V. Gupta, N. Chaudhary, R. Srivastava, G. D. Sharma, R. Bhardwaj and S. Chand, J. Am. Chem. Soc., 2011, 133, 9960-9963.

15. Y. Li, Y. Hu, Y. Zhao, G. Shi, L. Deng, Y. Hou and L. Qu, Adv. Mater., 2011, 23, 776-780.
16. X. Xu, R. Ray, Y. Gu, H. J. Ploehn, L. Gearheart, K. Raker and W. A. Scrivens, J. Am. Chem. Soc., 2004, 126, 12736-12737.
17. H. Liu, T. Ye and C. Mao, Angew. Chem. Int. Ed., 2007, 46, 6473-6475.
18. L. Tian, D. Ghosh, W. Chen, S. Pradhan, X. Chang and S. Chen, Chem. Mater., 2009, 21, 2803-2809.
19. D. Pan, J. Zhang, Z. Li and M. Wu, Adv. Mater., 2010, 22, 734-738.
20. S. Chen, J. Liu, M. Chen, X. Chen and J. Wang, Chem. Commun., 2012, 48, 7637-7639.
21. J. Peng, W. Gao, B. K. Gupta, Z. Liu, R. Romero-Aburto, L. Ge, L. Song, L. B. Alemany, X. Zhan and G. Gao, Nano Lett., 2012, 12, 844-849.
22. J. Zhou, C. Booker, R. Li, X. Zhou, T. K. Sham, X. Sun and Z. Ding, J. Am. Chem. Soc., 2007, 129, 744-745.
23. J. Lu, J. X. Yang, J. Wang, A. Lim, S. Wang and K. P. Loh, ACS Nano, 2009, 3, 2367-2375.
24. L. Zheng, Y. Chi, Y. Dong, J. Lin and B. Wang, J. Am. Chem. Soc., 2009, 131, 4564-4565.
25. H. Ming, Z. Ma, Y. Liu, K. Pan, H. Yu, F. Wang and Z. Kang, Dalton Trans., 2012, 41, 9526-9531.
26. A. B. Bourlinos, A. Stassinopoulos, D. Anglos, R. Zboril, V. Georgakilas and E. P. Giannelis, Chem Mater., 2008, 20, 4539-4541.
27. A. B. Bourlinos, A. Stassinopoulos, D. Anglos, R. Zboril, M. Karakassides and E. P. Giannelis, Small, 2008, 4, 455-458.
28. Y. Dong, J. Shao, C. Chen, H. Li, R. Wang, Y. Chi, X. Lin and G. Chen, Carbon, 2012, 50, 4738-4743.
29. B. Chen, F. Li, S. Li, W. Weng, H. Guo, T. Guo, X. Zhang, Y. Chen, T. Huang, X. Hong, S. You, Y. Lin, K. Zeng and S. Chen, Nanoscale, 2013, 5, 1967-1971.
30. S. Hu, K. Niu, J. Sun, J. Yang, N. Zhao and X. Du, J. Mater. Chem., 2009, 19, 484-488.
31. H. Zhu, W. Zhang and S. F. Yu, Nanoscale, 2013, 5, 1797-1802.
32. C. Zhu, J. Zhai and S. Dong, Chem. Commun., 2012, 48, 9367-9369.
33. S. Zhu, J. Zhang, L. Wang, Y. Song, G. Zhang, H. Wang and B. Yang, Chem. Commun., 2012, 48, 10889-10891.
34. Y. Yang, D. Wu, S. Han, P. Hu and R. Liu, Chem. Commun., 2013, 49, 4920-4922.
35. C. Wang, X. Wu, X. Li, W. Wang, L. Wang, M. Gu and Q. Li, J. Mater. Chem., 2012, 22, 15522-15525.
36. P.-C. Hsu and H.-T. Chang, Chem. Commun., 2012, 48, 3984-3986.
37. Q. Liang, W. Ma, Y. Shi, Z. Li and X. Yang, Carbon, 2013, 60, 421-428.
38. S. Zhu, Q. Meng, L. Wang, J. Zhang, Y. Song, H. Jin, K. Zhang, H. Sun, H. Wang and B. Yang, Angew. Chem. Int. Ed., 2013, 52, 3953-3957.
39. X. Q. Tian, C. M. Cheng, L. Qian, B. Z. Zheng, H. Y. Yuan, S. P. Xie, D. Xiao and M. M. F. Choi, J. Mater. Chem., 2012, 22, 8029-8035.
40. H. Zhu, X. Wang, Y. Li, Z. Wang, F. Yang and X. Yang, Chem. Commun., 2009, 5118-5120.
41. X. Wang, K. Qu, B. Xu, J. Ren and X. Qu, J. Mater. Chem., 2011, 21, 2445-2450.
42. L. Li, J. Ji, R. Fei, C. Wang, Q. Lu, J. Zhang, L. Jiang and J. Zhu, Adv. Funct. Mater., 2012, 22, 2971-2979.
43. L. Tang, R. Ji, X. Cao, J. Lin, H. Jiang, X. Li, K. S. Teng, C. M. Luk, S. Zeng, J. Hao and S. P. Lau, ACS Nano, 2012, 6, 5102-5110.
44. Y. Fang, S. Guo, D. Li, C. Zhu, W. Ren, S. Dong and E. Wang, ACS Nano, 2012, 6, 400-409.
45. J.-J. Liu, X.-L. Zhang, Z.-X. Cong, Z.-T. Chen, H.-H. Yang and G.-N. Chen, Nanoscale, 2013, 5, 1810-1815.
46. Y. Liu, C. Liu and Z. Zhang, J. Mater. Chem. C, 2013, 1, 4902-4907.
47. Y. Xu, M. Wu, X.-Z. Feng, X.-B. Yin, X.-W. He and Y.-K. Zhang, Chem.–Eur. J., 2013, 19, 6282-6288.
48. K. Qu, J. Wang, J. Ren and X. Qu, Chem.–Eur. J., 2013, 19, 7243-7249.
49. G. N. Naumov, M. B. Nilsson, T. Cascone, A. Briggs, O. Straume, L. A. Akslen, E. Lifshits, L. A. Byers, L. Xu, H.-k. Wu, P. Jänne, S. Kobayashi, B. Halmos, D. Tenen, X. M. Tang, J. Engelman, B. Yeap, J. Folkman, B. E. Johnson and J. V. Heymach, Clin. Cancer Res., 2009, 15, 3484-3494.
50. S. Park, J. An, R. D. Piner, I. Jung, D. Yang, A. Velamakanni, S. T. Nguyen and R. S. Ruoff, Chem. Mater., 2008, 20, 6592-6594.
51. J. Lee, K. Kim, W. I. Park, B. H. Kim, J. H. Park, T. H. Kim, S. Bong, C. H. Kim, G. Chae, M. Jun, Y. Hwang, Y. S. Jung and S. Jeon, Nano Lett, 2012, 12, 6078-6083.
52. Z. L. Wu, P. Zhang, M. X. Gao, C. F. Liu, W. Wang, F. Leng and C. Z. Huang, J. Mater. Chem. B, 2013, 1, 2868-2873.
53. J. Shang, L. Ma, J. Li, W. Ai, T. Yu and G. G. Gurzadyan, Sci. Rep., 2012, 2, 792-799.